Utilization of Halogen Bond in Lead Optimization: A Case Study of Rational Design of Potent Phosphodiesterase Type 5 (PDE5) Inhibitors[†]

Zhijian Xu,[‡,#] Zheng Liu,[§,#] Tong Chen,[‡,#] TianTian Chen,[‡] Zhen Wang,[‡] Guanghui Tian,[‡] Jing Shi,[§] Xuelan Wang,[§] Yunxiang Lu,[∥] Xiuhua Yan,[‡] Guan Wang,[‡] Hualiang Jiang,[‡] Kaixian Chen,[‡] Shudong Wang,[⊥] Yechun Xu,*,[‡] Jingshan Shen,*,[‡] and Weiliang Zhu*,[‡]

[‡]State key Laboratory of Drug Research, Shanghai Institute of Materia Medica, Chinese Academy of Sciences, 555 Zuchongzhi Road, Shanghai 201203, China

[§]Topharman Shanghai Co., Ltd., 1088 Chuansha Road, Shanghai 201209, China

[∥]Department of Chemistry, East China University of Science and Technology, 130 Meilong Road, Shanghai 200237, China

[⊥]School of Pharmacy, University of Nottingham, University Park, Nottingham NG7 2RD, U.K.

Ⓢ *Supporting Information*

ABSTRACT: For proof-of-concept of halogen bonding in drug design, a series of halogenated compounds were designed based on a lead structure as new inhibitors of phosphodiesterase type 5. Bioassay results revealed a good correlation between the measured bioactivity and the calculated halogen bond energy. Our X-ray crystal structures verified the existence of the predicted halogen bonds, demonstrating that the halogen bond is an applicable tool in drug design and should be routinely considered in lead optimization.

■ INTRODUCTION

Halogen bonding, a specific intermolecular interaction between a halogen atom and an electron-rich partner (O, N, or S), has been studied extensively using computational chemistry and has found a role in molecular engineering for material design.[1−5] Recently, it has also received recognition in biological systems as a distinct class of hydrogen-bond-like interactions, holding vast potential for applications in biological engineering.[6−12] Database surveys reveal that halogen bonding is a prevalent interaction between halogenated ligand and target protein,[9−12] and around 25% of the "top 200 brand name drugs by retail dollar in 2009" possess halogen atoms in their molecular structures. Therefore, halogens have a key role in drug development.

Here we present a case study to demonstrate how the introduction of halogen bonds between a ligand and its target can be applied to the structural optimization of lead compounds. The optimized lead compounds are phosphodiesterase type 5 (PDE5) inhibitors, being developed as potential drug candidates for the treatment of male erectile dysfunction and pulmonary arterial hypertension.[13]

Halogen bonding cannot be properly described by force field and scoring function, as halogen atoms are negatively charged as a whole but positively charged at certain regions of their atomic surface.[5,9] Consequently the interaction has not achieved a significant role in drug design and lead optimization. The fact that many drugs contain halogens in their molecular structure is not due to a rational computational approach but due to medicinal chemists' experience and intuition. For example, Valadares and co-workers identified a novel and previously unreported halogen bond in thyroid hormone.[14] Matter et al. demonstrated a successful utilization of C−Cl/C−Br···π interaction to enhance ligand−protein binding affinity, based on their long-term development of

serine protease factor Xa inhibitors.[7] More recently, Baumli et al. reported halogen bonds formed by DRB that are specific for the CDK9 kinase hinge region and contribute its high selectivity for the protein.[15] On the basis of an indication of a halogen bond between a 4-chlorophenyl moiety of a ligand and human cathepsin L, Hardegger et al. presented a systematic study on halogen bond in protein−ligand complexes.[11] Clearly, while the rational computational application of halogen bonding to drug design and lead optimization remains largely unexplored, a case study as proof-of-concept might help to convince and stimulate researchers to intentionally apply halogen bonding in drug development.

PDE5, which contains two cGMP-specific phosphodiesterases, bacterial adenylyl cyclase, FhLA transcriptional regulator (GAF) domains (GAF A and GAF B) in the N-terminal and a catalytic domain in the C-terminal, catalyzes the specific hydrolysis of cGMP to 5′-GMP. It is well-known as the target of sildenafil, an effective drug for the treatment of male erectile dysfunction and pulmonary arterial hypertension (Figure S1 in Supporting Information). Our group has synthesized a novel lead compound 6-ethyl-2-(5-(4-methylpiperazin-1-ylsulfonyl)-2-propoxyphenyl)pyrimidin-4(3*H*)-one (Figure 1a, X = H, **1**), structurally simpler but with weaker inhibitory activity than sildenafil (Table 1). Molecular docking of **1** to PDE5 (PDB entry 2H42) suggests that a halogen bond could be introduced between pyrimidinyl-5C of the ligand (Figure 1a) and the Y612 phenolate oxygen atom of the protein in the process of structural optimization (Figure 1b,c). We performed a PDB survey that supports the existence of O···X−C halogen bonds between

organic halogens and the phenolate oxygen of tyrosine (Figure S2 in Supporting Information). To further explore this concept, a hybrid quantum mechanics/molecular mechanics (QM/MM) method was employed to estimate the potential halogen bond strength between the halogenated **1** and PDE5, which gave a supportive prediction (ΔE, Table 1). The compounds were then synthesized and assayed for inhibitory activity against PDE5, and a good correlation was observed between the QM/MM derived binding energies and the experimentally determined bioactivity data (Table 1). To further validate the predicted halogen bonds, we determined the crystal structures of the corresponding complexes that clearly show that the halogen atoms at pyrimidinyl-5C moiety of ligands form halogen bonds with Y612 in PDE5. Thus, the study demonstrated that halogen bonding is a practicable tool for rational drug design and lead optimization.

■ RESULTS AND DISCUSSION

PDE5 Structure Used for Docking. Sildenafil has been widely studied, and several cocrystal structures with PDE5 have been resolved. In 2003 the structure of an inactive PDE5 in complex with sildenafil was determined by the multiwavelength anomalous dispersion method using Se-Met protein crystals (PDB entry
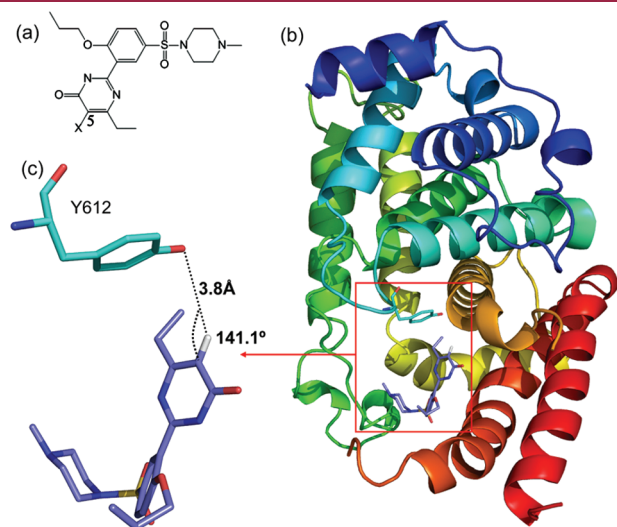
1UDT).[16] The H-loop in this structure was disordered, but a fully active catalytic domain of PDE5 containing a full length H-loop cocrystallized with sildenafil was recently resolved (PDB entry 2H42),[17] and this was used for docking for lead optimization in this study.

Designing New Halogenated Compounds. Figure 1 displays the docked complex structure of **1** and PDE5, revealing a geometrical pattern of the O···H−C with an angle of 141.1° and an interaction distance of 3.8 Å between Y612 oxygen atom and the 5-hydrogen atom of pyrimidinyl moiety of the lead compound **1** in the binding pocket (Figure 1c). With the concept of halogen bonding in mind, we realized that if the hydrogen atom is substituted by halogen atoms (Cl, Br, or I), a halogen bond might be introduced between the halogenated **1** and PDE5 to improve the bioactivity of the compounds. Hence, four halogenated derivatives of **1**, where X = F, Cl, Br, and I (namely, **2**, **3**, **4**, and **5**, respectively), were designed and subsequently docked to PDE5. The docked complexes show a halogen bonding interaction pattern between the newly designed halogenated ligands and the phenolate oxygen atom of Y612 in the binding pocket (Figure S3a and Table S1 in Supporting Information). A very similar binding mode between the designed ligands and sildenafil was observed, including two key interactions, i.e., hydrogen bonds with Q817 and a $\pi-\pi$ stacking interaction with F820 (Figure S3 in Supporting Information).[17]

Predicting Halogen Bond Energy. To further confirm the validity of this concept, a combined QM/MM scheme, viz., our own N-layered integrated molecular orbital and molecular mechanics (ONIOM), was employed to optimize the docked complexes and estimate the binding energy between the 5C-halogen atom and the phenolate O of Y612. To achieve this, the compounds and the side chain of Y612 are in the QM layer (Figure 2a−c), while the remainder of the protein, including Zn^{2+} and Mg^{2+}, is in the MM layer. Table 1 summarizes the optimized geometries of the halogen bonding systems and the calculated halogen bond energies. The optimized interaction distances and angles lie within the range of halogen bonding parameters found in biomolecules,[9,10] indicating the potential for halogen bonding between the designed compounds and PDE5 (Figure S4 in Supporting Information). Moving from F to H, Cl, Br, and I, a systematic increase in absolute value of the predicted halogen bond energy was observed, indicating that **3**, **4**, and **5** should show higher potency compared with lead **1** while **2** might be less active than **1** (Table 1).

Our calculations ignore entropy and solvation effects and, of course, have some limitations. Nevertheless, the conclusions derived may cast some light on the important role of halogen bond in rational drug design.

Figure 1. Structure and the binding mode of **1** (X = H) to PDE5 from the docking study. (a) Chemical structure of **1**. (b) The docked structure of **1**−PDE5 complex. PDE5 is shown in cartoon form with Y612 represented in stick form in the boxed area. **1** is also represented in the boxed area in stick form. (c) For clear visualization, the hydrogen bonding between 5C−H in **1** and Y612 in PDE5 extracted from (b) is shown.

Table 1. Predicted and Determined Parameters of Halogen Bonds and in Vitro Inhibitory Activity of the Compounds against PDE5

compd	X	$d(X\cdots O)$, Å		$\angle(C-X\cdots O)$, deg		ΔE, kcal/mol	IC_{50},[c] nM
		predicted	determined	predicted	determined		
1	H	3.24	NA[a]	129.5	NA[a]	−2.9	51.8 ± 12.1
2	F	3.50	3.85	127.7	150.7	−2.1	90.9 ± 22.4
3	Cl	3.43	3.60	126.9	141.0	−3.2	35.9 ± 11.5
4	Br	3.33	3.35[b]	132.6	149.2[b]	−3.3	13.3 ± 4.5
5	I	3.54	NA[a]	130.0	NA[a]	−4.5	7.2 ± 2.1

[a] NA: not available. [b] Data are the mean value of chain A and chain B in the asymmetric unit. [c] Data are the mean ± standard deviation (SD) of three independent experiments. Sildenafil was used as the control with IC_{50} of 3.3 ± 0.9 nM.
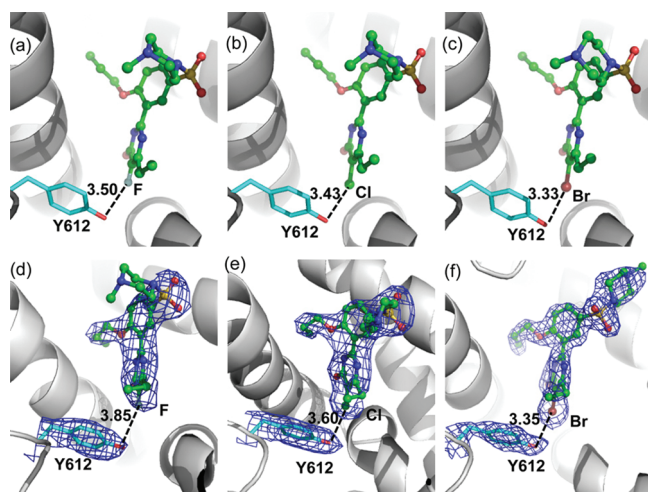
Figure 2. Optimized structures of PDE5 in complex with **2** (a), **3** (b), and **4** (c) at the ONIOM(B3LYP:AMBER) level, and the difference electron density maps contoured at 3.0σ for the complexes of PDE5 and **2** (d), **3** (e), and **4** (f) in the crystal structures, respectively.

Good Correlation between Predicted Halogen Bond Energy and Determined IC_{50}. The IC_{50} values determined experimentally with a scintillation proximity assay approach are shown in Table 1. It can be seen that the IC_{50} data of the compounds show good correlation with the predicted halogen bond strength, and **2** is the weakest inhibitor because of the totally electronegative surface of organic fluorines.[5,9] Our previous QM/MM computations on model protein kinase systems in complex with halogenated ligands also reproduced this strength order.[10] Moreover, we found that the activities of the five inhibitors (expressed as negative logarithm IC_{50}) correlate strongly with the binding energies with correlation coefficient $R = 0.93$ (Figure 3). The high quality of the correlation implies that the halogen bonding interactions contribute significantly to the increased activity. The most active compound **5** exhibits an IC_{50} of 7.2 nM, which is 13- and 7-fold more potent than **2** and **1**, respectively. Significantly, **5** is comparable in activity to sildenafil ($IC_{50} \approx 3.3$ nM), although it has a simpler structure.

Halogen Bond Validation by X-ray Crystallography. The 3D structures of the catalytic domain of PDE5 complexed with the inhibitors **2**, **3**, and **4** were determined by X-ray diffraction with resolutions of 2.65, 2.45, and 1.93 Å, respectively. The complex structures of PDE5 with **2** and **3** were obtained by soaking the inhibitors into the crystal of apo PDE5 with space group of $P3_121$ while that of PDE5 and **4** was solved by cocrystallization (space group $P2_12_12_1$) (Table S2 in Supporting Information). Figure 2d—f shows the difference electron density maps contoured at 3.0σ for the three inhibitors, which clearly demonstrated that the halogenated inhibitors bind to the catalytic domain of PDE5. Our determined distances in the crystal structures between the phenolate oxygen atom of Y612 and the halogen atoms in **2** and **3**, viz. 3.60 and 3.35 Å, are in excellent agreement with the optimized distances by QM/MM approach, viz. 3.43 and 3.33 Å, respectively, verifying that halogen bonds do exist between PDE5 and the two newly designed and synthesized inhibitors. Superimposition of the crystal structures and the docking conformations (or the QM/MM optimized conformations) of the inhibitors resulted in rmsd of 1.13 (0.83), 0.85 (1.12), and 2.72 (2.54) Å for **2**, **3**, and **4**, respectively, indicating that docking
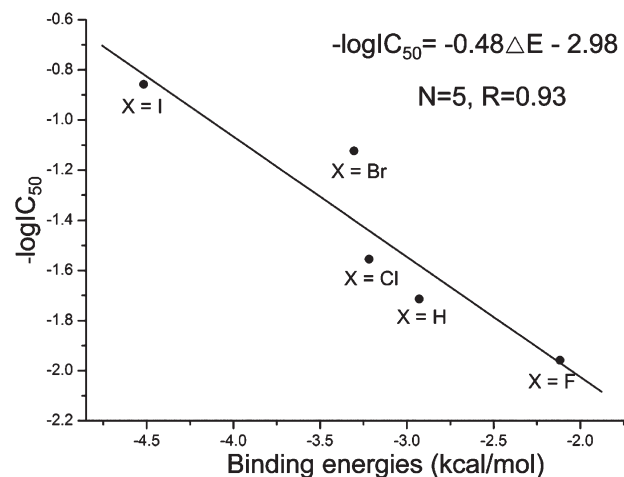

Figure 3. Plot of $-\log IC_{50}$ versus halogen bond energies for the side chain of Y612.

protocol and model predict quite well the binding of the three inhibitors into PDE5. It was observed that the methylpiperazine group in **4** adopts a different conformation from the docking result due to a crystal packing effect. When the methylpiperazine group is excluded, the rmsd of the inhibitor between the crystal structure and the docking conformation (or the QM/MM optimized conformation) of **4** is 1.23 (1.10) Å.

Although the halogen substitution at the C5 pyrimidinyl moiety may lead to a change in lipophilic or space filling interactions, the three X-ray structures demonstrated that the introduction of large halogens does not change the position of Y612. Thus, the shorter distances between the negatively charged phenolate oxygen atom of Y612 and the overall negatively charged Cl/Br should be logically attributed mainly to the halogen bonding between the O and Cl/Br, while the longer distance between the O and F is due to the repulsion between them. In other words, the attraction between the electronegative O of Y612 and partially electropositive halogen atoms Cl and Br around their cap areas along C—X axis,[10] namely, halogen bond, is the main cause for their increased inhibitory activity against PDE5. The small effect of the introduction of halogens on IC_{50} may be attributed to the weak halogen bonds with O···X distances close to the sum of vdW radii (Table 1). Therefore, a more careful design to form stronger halogen bond in other systems may lead to more significant improvement in the bioactivity for lead optimization.

■ CONCLUSION

We have systematically explored the power of halogen bonding in the context of computational rational drug design. A series of halogenated compounds as potential PDE5 inhibitors were designed, prepared, and evaluated. The experimentally determined bioactivities correlated well with the halogen bond energies predicted at the QM/MM level between the new inhibitors and the enzyme. The X-ray crystal structures of PDE5 complexed with the new inhibitors verified the existence of the predicted halogen bonds, viz., the bonds between the phenolate oxygen atom of Y612 and Cl/Br in the ligands. In addition, one of the newly designed compounds, **5**, shows an activity comparable to that of sildenafil. Therefore, this study demonstrated that the

Scheme 1. Syntheses of Pyrimidin-4(3H)-one 1 and 5-Halopyrimidin-4(3H)-ones 2−5[a]
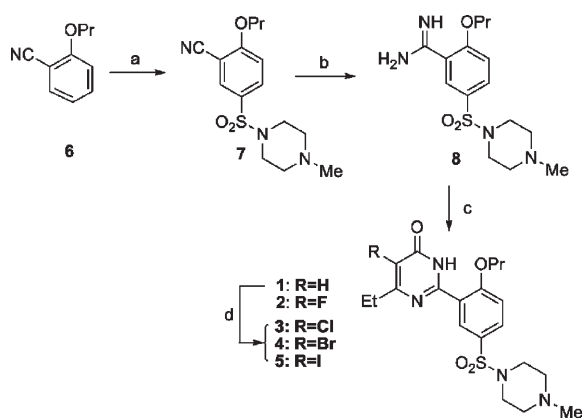
[a] Reagents and conditions: (a) (i) HSO3Cl, 0 °C; (ii) N-methylpiperazine, Et3N, DCM, 0 °C; (b) LiHMDS, THF, room temp; (c) K2CO3, DMF, 100 °C, methyl 3-oxopentanoate or methyl 2-fluoro-3-oxopentanoate; (d) for **3**, Cl2 (g), Et3N, DCM, 0 °C; for **4**, Br2, Et3N, DCM, 0 °C; for **5**, I2, AgNO3, MeOH, room temp.

halogen bond is a practical and effective tool in drug design and lead optimization.

■ EXPERIMENTAL SECTION

Molecular Docking. The compounds were docked to PDE5 (PDB entry 2H42) using Glide in its XP mode in a standard procedure. The water molecules were removed, while the zinc and magnesium ions were retained with charge +2, respectively. The compounds were sketched by Maestro and processed by LigPrep under its default parameters. The docked conformation of the compound with the lowest energy was selected for further study.

QM/MM Calculation Procedure. In brief, the systems studied were divided into two layers: the small molecule and the side chain of Y612 were placed in the QM layer, while the rest of the protein was in the MM layer. For the QM layer, the B3LYP/6-31G(d) method was applied for **1**−**4**, but the B3LYP/lanl2dz was used for **5**.[10] The MM layer of the system was modeled with the AMBER force field. Single-point energy computations were performed using MP2/6-311+G(d) for **1**−**4** and MP2/6-311+G(d) plus SDD for **5**. The binding energies between the inhibitors and the residue Y612 were computed via the protocol as described previously.[10]

Chemistry. **1** and **2** were prepared from the starting material *o*-propoxybenzonitrile following the procedure in Scheme 1. Halogenation of **1** resulted in the corresponding 5-halopyrimidinone derivatives **3**−**5**.

All melting points were determined on a Buchi apparatus and are uncorrected. ^{1}H NMR spectra were determined using a Mercury 300 MHz, FT NMR spectrometer. HRMS were performed on a Finnigan MAT95 mass spectrometer, and ESIMS was carried out on a Finnigan LCQdeca mass spectrometer. Reaction solvents were purchased and used without further purification. HPLC conditions were as follows: column, YMC-Pack CN 5 μM, 4.6 mm × 250 mm; solvent system, (A) MeCN; (B) 0.02 M KH2PO4 (pH 6.0); step gradient, time 0, 30% A; time 20 min, 70% A; stop time, 25 min; flow rate 1.0 mL/min; UV detection, 220 nm; injection volume, 5 μL; temperature, 30 °C. The purity of all target compounds was >95% as confirmed by HPLC.

6-Ethyl-2-[2-propoxy-5-(4-methyl-1-piperazinylsulfonyl)-phenyl]pyrimidin-4(3H)-one (1). A mixture of 5-(4-methylpiperazin-1-ylsulfonyl)-2-propoxybenzimidamide **8** (1.2 g, 3.2 mmol), methyl

3-oxopentanoate (0.5 g, 3.8 mmol), and potassium carbonate (0.9 g, 6.4 mmol) in DMF (10 mL) was stirred at 100 °C for 4 h. The mixture was then cooled to room temperature and taken up in water (50 mL) and DCM (50 mL). The organic layer was separated, and the aqueous layer was extracted further with DCM (50 mL). The combined organic layers were dried (Na2SO4) and concentrated. The residue was purified by flash column chromatography. After crystallization from EtOAc, **1** was obtained as white crystals (0.81 g, 60%): mp 151−152 °C. HPLC purity 98.2%; t_R= 16.3 min. ^{1}H NMR (DMSO-d_6, 300 MHz) δ: 7.89 (d, J = 2.4 Hz, 1H), 7.84 (dd, J_1 = 2.4 Hz, J_2 = 8.7 Hz, 1H), 7.39 (d, J = 8.7 Hz, 1H), 4.15 (t, J = 6.3 Hz, 2H), 2.89 (br, 4H), 2.45 (q, J = 7.5 Hz, 2H), 2.36 (br, 4H), 2.16 (s, 3H), 1.75 (m, 2H), 1.13 (t, J = 7.5 Hz, 3H), 0.96 (t, J = 7.5 Hz, 3H). HRMS calcd [M + Na]+ for C20H28N4O4NaS 443.1729, found 443.1736.

5-Fluoro-6-ethyl-2-[2-propoxy-5-(4-methyl-1-piperazinyl-sulfonyl)phenyl]pyrimidin-4(3H)-one (2). 2 was prepared in 72% yield from **8** and methyl 2-fluoro-3-oxopentanoate following a similar procedure to that described for **1**: mp 163−164 °C. HPLC purity 98.3%; t_R= 10.2 min. ^{1}H NMR (CDCl3, 300 MHz) δ: 8.80 (d, J = 2.1 Hz, 1H), 7.86 (dd, J_1 = 2.1 Hz, J_2 = 8.7 Hz, 1H), 7.16 (d, J = 8.7 Hz, 1H), 4.26 (t, J = 6.6 Hz, 2H), 3.09 (br, 4H), 2.74 (q, J = 7.5 Hz, 2H), 2.51 (br, 4H), 2.28 (s, 3H), 2.03 (m, 2H), 1.28 (t, J = 7.5 Hz, 3H), 1.15 (t, J = 7.5 Hz, 3H). HRMS calcd [M + Na]+ for C20H27N4O4NaSF 461.1635, found 461.1630.

5-Chloro-6-ethyl-2-[2-propoxy-5-(4-methyl-1-piperazinyl-sulfonyl)phenyl]pyrimidin-4(3H)-one (3). Chlorine gas was bubbled into an ice-cold solution of **1** (100 mg, 0.24 mmol) and pyridine (40 μL, 0.5 mmol) in DCM (10 mL) for 1 min. The resulting mixture was washed with 1 N Na2S2O3 (aq) (5 mL) and water (5 mL). The organic layer was dried (Na2SO4) and concentrated in vacuo. After crystallization from EtOAc, **3** was obtained as white crystals (93 mg, 85%): mp 188−189 °C. HPLC purity 98.3%; t_R= 10.1 min. ^{1}H NMR (CDCl3, 300 MHz) δ: 11.25 (1H, br), 8.85 (d, J = 2.1 Hz, 1H), 7.87 (dd, J_1 = 2.1 Hz, J_2 = 8.7 Hz, 1H), 7.16 (d, J = 8.7 Hz, 1H), 4.27 (t, J = 6.6 Hz, 2H), 3.08 (br, 4H), 2.85 (q, J = 7.5 Hz, 2H), 2.49 (br, 4H), 2.27 (s, 3H), 2.03 (m, 2H), 1.29 (t, J = 7.5 Hz, 3H), 1.15 (t, J = 7.5 Hz, 3H). HRMS calcd [M + Na]+ for C20H27N4O4NaSCl 477.1339, found 477.1339.

5-Bromo-6-ethyl-2-[2-propoxy-5-(4-methyl-1-piperazinyl-sulfonyl)phenyl]pyrimidin-4(3H)-one (4). Bromine (40 mg, 0.27 mmol) was added to an ice-cold solution of **1** (100 mg, 0.24 mmol) and pyridine (22 μL, 0.27 mmol) in DCM (10 mL). The mixture was stirred for 15 min at 0 °C and washed with 1 N Na2S2O3 (5 mL) and water (5 mL). The organic layer was dried (Na2SO4) and concentrated. After crystallization from EtOAc, **4** was obtained as white crystals (107 mg, 90%): mp 182−183 °C. HPLC purity 98.9%; t_R= 10.0 min. ^{1}H NMR (CDCl3, 300 MHz) δ: 11.12 (1H, br), 8.86 (d, J = 2.1 Hz, 1H), 7.88 (dd, J_1 = 2.1 Hz, J_2 = 8.7 Hz, 1H), 7.16 (d, J = 8.7 Hz, 1H), 4.27 (t, J = 6.6 Hz, 2H), 3.09 (br, 4H), 2.88 (q, J = 7.5 Hz, 2H), 2.50 (br, 4H), 2.28 (s, 3H), 2.03 (m, 2H), 1.29 (t, J = 7.5 Hz, 3H), 1.15 (t, J = 7.5 Hz, 3H). HRMS calcd [M + Na]+ for C20H27N4O4NaSBr 521.0834, found 521.0834.

5-Iodo-6-ethyl-2-[2-propoxy-5-(4-methyl-1-piperazinyl-sulfonyl)phenyl]pyrimidin-4(3H)-one (5). Iodine (254 mg, 1 mmol) was added to a solution of **1** (420 mg, 1 mmol) and silver nitrate (170 mg, 1 mmol) in MeOH (10 mL) at 0 °C. The mixture was stirred at room temperature for 30 min. After filtration, the filtrate was poured into water (25 mL) and extracted with DCM (20 mL). The organic layer was washed with 1 N Na2S2O3 (5 mL) and water (5 mL), dried, and concentrated. After crystallization from EtOAc, **5** was obtained as white crystals (410 mg, 75%): mp 193−194 °C. HPLC purity 97.5%; t_R = 12.2 min. ^{1}H NMR (CDCl3, 300 MHz) δ: 11.12 (1H, br), 8.88 (d, J = 2.1 Hz, 1H), 7.88 (dd, J_1 = 2.1 Hz, J_2 = 8.7 Hz, 1H), 7.16 (d, J = 8.7 Hz, 1H), 4.27 (t, J = 6.6 Hz, 2H), 3.10 (br, 4H), 2.92 (q, J = 7.5 Hz, 2H), 2.52 (br, 4H), 2.30 (s, 3H), 2.03 (m, 2H), 1.28

(t, J = 7.5 Hz, 3H), 1.16 (t, J = 7.5 Hz, 3H). HRMS calcd $[M + Na]^+$ for $C_{20}H_{27}N_4O_4NaSI$ 569.0695, found 569.0704.

Bioassay. The synthesized compounds **1**−**5** were evaluated for their inhibitory activities against PDE5 isolated from rabbit platelet using $[^3H]$cGMP SPA kit detailed in the Supporting Information.

■ ASSOCIATED CONTENT

ⓢ Supporting Information.   Figures S1−S4, Tables S1 and S2, additional information on analytical and bioassay data for **1**−**5**, **7**, and **8**, protein purification and crystallization, and structure determination and refinement. This material is available free of charge via the Internet at http://pubs.acs.org.

Accession Codes

†The atomic coordinates 3SHY, 3SHZ, and 3SIE have been deposited in the Protein Data Bank.

■ AUTHOR INFORMATION

Corresponding Author

*For Y.X.: phone, +86 21 50801267; e-mail, ycxu@mail.shcnc.ac.cn. For J.S.: phone, +86 21 20231962; e-mail, jsshen@mail.shcnc.ac.cn. For W.Z.: phone, +86 21 50805020; fax, +86 21 50807088; e-mail, wlzhu@mail.shcnc.ac.cn.

Author Contributions

#These authors contributed equally to this study.

■ ACKNOWLEDGMENT

■ ABBREVIATIONS USED

GAF, cGMP-specific phosphodiesterase, bacterial adenylyl cyclase, FhLA transcriptional regulator; ONIOM, our own N-layered integrated molecular orbital and molecular mechanics; PDB, Protein Data Bank; PDE5, phosphodiesterase type 5; QM/MM, quantum mechanics/molecular mechanics

■ REFERENCES

(1) Metrangolo, P.; Neukirch, H.; Pilati, T.; Resnati, G. Halogen bonding based recognition processes: a world parallel to hydrogen bonding. *Acc. Chem. Res.* **2005**, *38*, 386–395.

(2) Politzer, P.; Murray, J. S.; Clark, T. Halogen bonding: an electrostatically-driven highly directional noncovalent interaction. *Phys. Chem. Chem. Phys.* **2010**, *12*, 7748–7757.

(3) Cavallo, G.; Metrangolo, P.; Pilati, T.; Resnati, G.; Sansotera, M.; Terraneo, G. Halogen bonding: a general route in anion recognition and coordination. *Chem. Soc. Rev.* **2010**, *39*, 3772–3783.

(4) Bertani, R.; Sgarbossa, P.; Venzo, A.; Lelj, F.; Amati, M.; Resnati, G.; Pilati, T.; Metrangolo, P.; Terraneo, G. Halogen bonding in metal-organic-supramolecular networks. *Coord. Chem. Rev.* **2010**, *254*, 677–695.

(5) Politzer, P.; Lane, P.; Concha, M. C.; Ma, Y.; Murray, J. S. An overview of halogen bonding. *J. Mol. Model.* **2007**, *13*, 305–311.

(6) Voth, A. R.; Khuu, P.; Oishi, K.; Ho, P. S. Halogen bonds as orthogonal molecular interactions to hydrogen bonds. *Nat. Chem.* **2009**, *1*, 74–79.

(7) Matter, H.; Nazare, M.; Gussregen, S.; Will, D. W.; Schreuder, H.; Bauer, A.; Urmann, M.; Ritter, K.; Wagner, M.; Wehner, V. Evidence for C−Cl/C−Br···pi interactions as an important contribution to protein−ligand binding affinity. *Angew. Chem., Int. Ed.* **2009**, *48*, 2911–2916.

(8) Voth, A. R.; Hays, F. A.; Ho, P. S. Directing macromolecular conformation through halogen bonds. *Proc. Natl. Acad. Sci. U.S.A.* **2007**, *104*, 6188–6193.

(9) Auffinger, P.; Hays, F. A.; Westhof, E.; Ho, P. S. Halogen bonds in biological molecules. *Proc. Natl. Acad. Sci. U.S.A.* **2004**, *101*, 16789–16794.

(10) Lu, Y.; Shi, T.; Wang, Y.; Yang, H.; Yan, X.; Luo, X.; Jiang, H.; Zhu, W. Halogen bonding—a novel interaction for rational drug design? *J. Med. Chem.* **2009**, *52*, 2854–2862.

(11) Hardegger, L. A.; Kuhn, B.; Spinnler, B.; Anselm, L.; Ecabert, R.; Stihle, M.; Gsell, B.; Thoma, R.; Diez, J.; Benz, J.; Plancher, J. M.; Hartmann, G.; Banner, D. W.; Haap, W.; Diederich, F. Systematic investigation of halogen bonding in protein−ligand interactions. *Angew. Chem., Int. Ed.* **2011**, *50*, 314–318.

(12) Parisini, E.; Metrangolo, P.; Pilati, T.; Resnati, G.; Terraneo, G. Halogen bonding in halocarbon−protein complexes: a structural survey. *Chem. Soc. Rev.* **2011**, *40*, 2267–2278.

(13) Prasad, S.; Wilkinson, J.; Gatzoulis, M. A. Sildenafil in primary pulmonary hypertension. *N. Engl. J. Med.* **2000**, *343*, 1342.

(14) Valadares, N. F.; Salum, L. B.; Polikarpov, I.; Andricopulo, A. D.; Garratt, R. C. Role of halogen bonds in thyroid hormone receptor selectivity: pharmacophore-based 3D-QSSR studies. *J. Chem. Inf. Model.* **2009**, *49*, 2606–2616.

(15) Baumli, S.; Endicott, J. A.; Johnson, L. N. Halogen bonds form the basis for selective P-TEFb inhibition by DRB. *Chem. Biol.* **2010**, *17*, 931–936.

(16) Sung, B. J.; Hwang, K. Y.; Jeon, Y. H.; Lee, J. I.; Heo, Y. S.; Kim, J. H.; Moon, J.; Yoon, J. M.; Hyun, Y. L.; Kim, E.; Eum, S. J.; Park, S. Y.; Lee, J. O.; Lee, T. G.; Ro, S.; Cho, J. M. Structure of the catalytic domain of human phosphodiesterase 5 with bound drug molecules. *Nature* **2003**, *425*, 98–102.

(17) Wang, H.; Liu, Y.; Huai, Q.; Cai, J.; Zoraghi, R.; Francis, S. H.; Corbin, J. D.; Robinson, H.; Xin, Z.; Lin, G.; Ke, H. Multiple conformations of phosphodiesterase-5: implications for enzyme function and drug development. *J. Biol. Chem.* **2006**, *281*, 21469–21479.